33. M. R. Grimmett, in "Comprehensive Heterocyclic Chemistry," Vol. 5, A. R. Katritzky and C. W. Rees, Editors, p. 375 and 417, Pergamon Press, Oxford (1984).
34. R. S. Nicholson and I. Shain, *Anal. Chem.*, **36,** 706 (1964).
35. A. J. Bard and L. R. Faulkner, "Electrochemical Methods: Fundamentals and Applications," p. 218, John Wiley and Sons, Inc., New York (1980).
36. R. E. Hester and K. P. J. Williams, *J. Raman Spectrosc.*, **13,** 91 (1982).
37. B. L. Barton and G. K. Fraenkel, *J. Chem. Phys.*, **41,** 1455 (1964).
38. D. W. Schieser and P. Zvirblis, *ibid.*, **35,** 2237 (1962).
39. D. N. Bailey, D. K. Roe, and D. M. Hercules, *J. Am. Chem. Soc.*, **90,** 6291 (1968).
40. M. Berndt and W. Woznicki, *Acta Phys. Polon.*, **A43,** 101 (1973).
41. D. N. Bailey, D. M. Hercules, and D. K. Roe, *This Journal*, **116,** 190 (1969).
42. A. J. Bard and L. R. Faulkner, "Electrochemical Methods: Fundamentals and Applications," Chap. 11, John Wiley and Sons, New York (1980).
43. A. Albert, "Heterocyclic Chemistry," Chap. 11, pp. 376-419, Athlone Press, London (1968).
44. S. P. Zingg, G. P. Smith, and A. S. Dworkin, In preparation.
45. F. Gerson, "High Resolution E.S.R. Spectroscopy," p. 13, John Wiley and Sons, Ltd., Weinheim (1970).
46. A. Carrington and J. dos Santos-Veiga, *Mol. Phys.*, **5,** 21 (1962).

Electron Transfer Through Thin Anodic Oxide Films during the Oxygen Evolution Reactions at Pt Electrodes

I. Acid Solutions

A. Damjanovic

Allied-Signal, Incorporated, Research and Technology, Morristown, New Jersey 07962-1021

V. I. Birss*

Department of Chemistry, University of Calgary, Calgary, Alberta, Canada T2N 1N4

D. S. Boudreaux

Allied-Signal, Incorporated, Research and Technology, Morristown, New Jersey 07962-1021

ABSTRACT

The electron transfer process, which occurs during oxygen evolution at Pt electrodes from water molecules in the double layer, is analyzed. The process proceeds by electron tunneling through an insulating anodic Pt oxide film to the underlying Pt metal as oxygen is evolved. The rate equation for the reaction is based on a model of quantum tunneling through a barrier which is a composite of both the oxide film and the inner Helmholtz layer. For a barrier thickness of 10 Å, the probability of tunneling decreases by a factor of three as the electrode potential increases from 1.29 to 2.01 V *vs.* RHE. This decrease is small when compared to the observed, ca. 10^6, increase in current density for the same potential span. The current density is controlled primarily by the distribution of electron energy states of the reacting donor species which are water molecules in the inner Helmholtz plane. At a constant potential, the tunneling probability depends exponentially on the thickness of the potential barrier, and therefore the rate of the oxygen evolution reaction is strongly dependent on the Pt oxide film thickness.

Although platinum is a poor catalyst for the oxygen evolution reaction (OER) compared to various metal oxide electrodes, it has served as a model electrode in studies of the mechanism of the OER and of catalytic factors affecting reaction rates. Despite this, the state of knowledge of the mechanism of the OER is not satisfactory. This is partly because of the variance in the kinetic data reported in the literature (1-12), as well as the complexity of the processes occurring at this electrode during oxygen evolution.

In acid solutions, a linear E-log i relationship has been reported for OER with a Tafel slope of approximately $2.3(2RT)/F$ (~120 mV at room temperature) for four to six decades of the logarithm of current density (1-3, 6-11). This slope has been associated with the first electron transfer process being the rate-determining step with H_2O in the double layer as the reactant (1, 2, 5, 10, 13), *i.e.*, in a simple form

$$S + H_2O \rightarrow S \ldots (OH{-}H)^+ + e^- \qquad [1]$$

Here, S represents a site at the oxide film covered electrode surface. Brackets around the products in the step indicate that the nature of the products in a rate-determining step, in principle, is not known. Although the pH dependence for this as the rate-determining step is expected to be zero, *i.e.*, the rate of the reaction at any constant potential *vs.* a pH-independent reference electrode should not vary with pH of solution, evidence has accumulated which shows that $(d \log i/d\mathrm{pH})_E$ is not zero but rather 1/2 (1, 4, 7, 13, 14). Such a dependence leads to the fractional reaction order with respect to H_3O^+.

Furthermore, it is known that a thin (10-15 Å), insulating Pt oxide film covers the electrode surface in the potential region of the OER (13, 15-19) and that its presence hinders the rate of the OER (1, 4, 7, 13, 19). The rate decreases exponentially with the thickness of the oxide film (1, 4, 13). Thus, the following rate equation describes the kinetics of the OER in acid solutions (13)

$$\begin{aligned} i &= A[H_3O^+]^{-1/2} \exp(-mFq/(2RT)] \exp[FE/(2RT)] \\ &= A[H_3O^+]^{-1/2} \exp[-\delta d] \exp[FE/(2RT] \end{aligned} \qquad [2]$$

Here, q is the charge density equivalent to the oxide film thickness, d, and m $[=(dE/dq)_i]$ and d are experimentally available parameters (1, 4, 13). The electrode potential, E, is given with respect to a pH-independent reference elec-

* Electrochemical Society Active Member.

trode. The pre-exponential factor, A, depends on the choice of the reference electrode but is pH independent.

An important characteristic of the OER at Pt is that a constant Tafel slope [$2.3(2RT)/F$] can be observed only when q, and hence d, is constant. This is achieved when an electrode is anodically pretreated, for instance with a constant current, i_p, for some time (*e.g.*, 2 h), and the E-log i relationship is subsequently determined at $i < i_p$ (1, 6, 7). During such a pretreatment, an oxide film grows uniformly over the electrode surface according to the high field assisted ion migration mechanism of Cabrera and Mott to a thickness, d, of about 10 Å (15-18). When E-log i data are subsequently determined at $i < i_p$, the field within the oxide film sharply decreases and oxide growth essentially ceases (1, 7). E-log i measurements for the OER are then taken at a constant d. The variance in the kinetic data in the literature for the OER at Pt, particularly when Tafel slopes are reported to be changing with potential even over a narrow range of current density (4), is probably related to a variable thickness of the oxide film during the E-log i measurements.

Another characteristic of the OER at Pt electrodes is that the reaction order with respect to hydrogen ions is negative and fractional, *i.e.*, −1/2. This fractional order cannot be accounted for by any common approach in electrode kinetics.

In this paper, an analysis is given of the kinetics of the OER in acid solutions, and a model for charge transfer is suggested which accounts for the exponential dependence of the rates on electrode potential and on oxide film thickness, as well as for the observed fractional reaction order with respect to H_3O^+. It is based on a dual barrier model at the metal/oxide film/solution interface and electron tunneling through the oxide film.

Dual Barrier Model of the Metal/Oxide Film/Solution Interface

The fractional reaction order with respect to H^+ in Eq. [2] is explained in terms of a dual barrier model. The dual barrier consists of an inner zone comprised of the oxide film plus the inner Helmholtz layer (IHL), in series with the outer zone, the outer Helmholtz layer (OHL) (1, 13). In this model, the first electrochemical step involving electron transfer from energetically activated water molecules in the inner Helmholtz plane (IHP) to the underlying metal is proposed to be the rate-determining step. Charge transfer (of H^+) across the outer barrier is fast, *i.e.*, at all potentials a quasiequilibrium exists between protons at the IHP and those at the outer Helmholtz plane (OHP) and solution. The diffuse double layer is ignored for concentrated solutions. Thus, only the Galvani potential difference across the inner barrier, $\Delta\phi_{ib}$, controls the reaction rate of the OER; as the electrode potential increases, only $\Delta\phi_{ib}$ increases, while the Galvani potential difference across the OHL, $\Delta\phi_{ob}$, remains constant (at a given pH). As pH increases, $\Delta\phi_{ib}$ remains constant for a given current density and thickness of the oxide film, while $\Delta\phi_{ob}$ decreases 60 mV as pH increases one unit (1). A schematic representation of the potential distributions across the barriers is shown in Fig. 1 for two current density and two pH values. In this figure, E is the potential of the Pt electrode *vs.* a pH-independent reference electrode. E_o denotes the potential at the IHP *vs.* the same reference electrode [cf. (1, 13, 20)], and therefore[1]

$$E - E_o \equiv \Delta E_{ib} = \Delta\phi_{ib} = \phi_M - \phi_{IHP} \qquad [3]$$

Potential difference $E - E_o$ may be called the operative potential difference as only this difference determines the current density.

Reaction Path for the OER

The initial steps in the reaction path for the OER, based on the dual barrier model, is represented by reactions [4] and [5], where the subscripts indicate the location of the species, and M stands for the Pt metal electrode, *i.e.*

$$2H_2O_{IHP} \rightarrow (OH \ldots H_3O)^+_{IHP} + e^-_M \qquad [4]$$

$$(OH \ldots H_3O)^+_{IHP} + H_2O_{OHP} \leftrightarrow H_2O_{IHP} + OH_{IHP} + H_3O^+_{OHP} \qquad [5]$$

No particular significance should be attached to the details in the structure of the reaction products in the first step, as well as in the structures of the reactants and products in the second, fast chemical step, which is in a quasiequilibrium. These equatives are meant to indicate that charge transfer across the OHL occurs via a fast proton transfer step.

Reaction [4] is the slow electrochemical step that proceeds at a rate which depends on $\Delta\phi_{ib}$, while reaction [5] is independent of this potential. At a given film thickness, the rate equation for reaction [4] as the rate-determining step is given by [cf. (1, 13)]

$$\begin{aligned} i &= k'' \exp[\beta F \Delta\phi_{ib}/(RT)] \\ &= k' \exp[\beta F(E - E_o)/(RT)] \end{aligned} \qquad [6]$$

where β is the symmetry factor (~1/2), and k'' and k' contain the pre-exponential factor A from Eq. [2], and the exponential term which depends on the oxide film thickness. It does not contain the proton concentration in solution. Factors k' and k'' may differ in chemical potentials of electrons in the metal, IHP and OHP, as briefly discussed in footnote 1. This is not important, however, for the analysis of the kinetics presented in this paper.

E_o is experimentally obtained; it is given by

$$E_o = E_{o,pH=0} - \frac{2.3RT}{F}\,pH \qquad [7]$$

where $E_{o,pH=0}$ ~0.96 V *vs.* SHE (1, 13, 17-19, 20). When E_o is substituted into Eq. [6], the rate equation with the negative and fractional reaction order of −1/2 with respect to H_3O^+ is obtained.

Since the growth of the Pt oxide film obeys the formalism of the Cabrera-Mott model of high field ionic migration through the film (13, 16-19, 20), it follows that the oxide film, which is only about 10-15 Å thick (17-19), is a poor electronic conductor. Because the OER occurs at very high rates, electrons needed for the reaction must tunnel through the oxide film from donor states in solution to the underlying metal. It is important to distinguish the present model from those based on electronically conductive oxides in which electrons required for an electrochemical re-

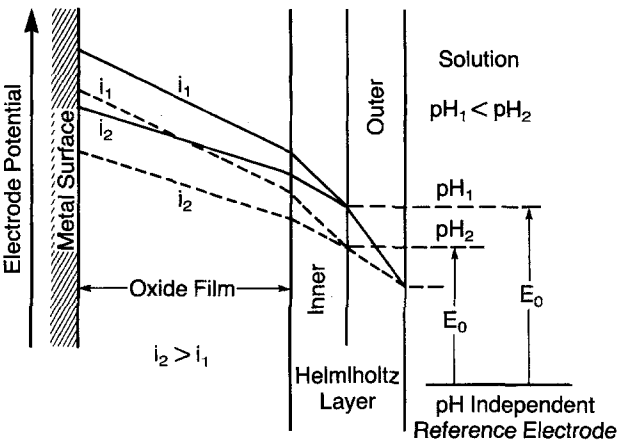

Fig. 1. A schematic representation of the model of the potential distribution across the metal/oxide film/solution interface at two cd's and two pH's. For the same cd, the potential difference across the OF and IHL is the same at different pH's. The potential difference across the OHL, however, decreases 60 mV as pH increases one unit. At the same pH, the potential difference across the OF and IHL increases by 120 mV as the cd increases ten times, while the potential difference across the OHL remains the same. Potentials within the oxide film at currents i_1 and i_2 are indicated. Broken line: pH_2; full line: pH_1. E is the potential of Pt electrode *vs.* a pH-independent reference electrode.

[1] For simplicity, in the relation [3], differences in chemical potentials of electrons in the metal, IHP and OHP are omitted. They will, as constant terms, appear in the pre-exponential factor. This, however, will not affect the derivation of the rate equation for the OER and the conclusion drawn from it.

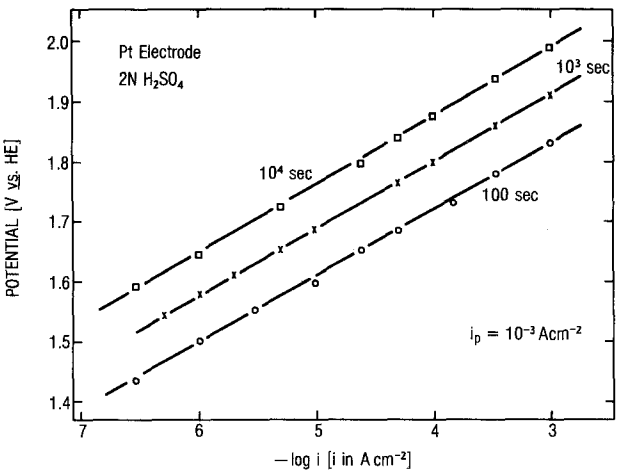

Fig. 2. Typical Tafel lines for oxygen evolution (1, 6, 7).

action, such as the OER, migrate through the oxide film [cf. (21-23)].

Electron Tunneling through Thin Oxide Films

A rate equation based on quantum mechanical concepts of electron tunneling through an insulating barrier can be derived for the suggested reaction scheme for the OER. Such a rate equation must be consistent with four major observations discussed above. First, it must yield a Tafel slope close to $2.3(2RT)/F$ for over six decades of current density without any noticeable deviation from linearity (see Fig. 2). This is equivalent to the requirement that Tafel slopes are independent of electrode potential, *i.e.*, $\beta \neq f(E)$. Second, the logarithmic dependence of the rate on oxide film thickness must follow from such a derivation. Third, the negative and fractional reaction order (−1/2) with respect to H_3O^+ must be obtained. Four, the rates should be consistent with the relatively low values of the exchange current densities found for the OER at Pt electrodes.

In this work, we use the basic concepts of Gurney (24) and Gerischer (25), and the developments of Bockris and co-workers (26-28), concerning the tunneling process at metal/solution interfaces. The present paper extends these to electron tunneling through a composite barrier consisting of a metal oxide film and the IHL. In a similar study, Vetter and Schultze (29) derived a rate equation in which Tafel slopes increase with electrode potential. In addition, their rate equation does not satisfactorily account for the observed pH dependence of the OER.

The electron tunneling current at a given electrode potential is usually written in the form (24-30)

$$i(E) = \nu\kappa \frac{kT}{h} e_o \int_\epsilon N(\epsilon)S(\epsilon)[1 - f(\epsilon)]W(\epsilon,d)d\epsilon \qquad [8]$$

Here, κ is the transmission coefficient, ν the stoichiometry number, and e_o the electron charge. Other symbols in front of the integral have their usual significance. $N(\epsilon)$ is the distribution of electron energy levels, ϵ, for donor species. Donor species are considered to be H_2O molecules, or their aggregation, in the IHP (see reactions [4] and [5]). $S(\epsilon)$ is the density of electron states in the metal, and $[1 - f(\epsilon)]$, where $f(\epsilon)$ is the Fermi distribution function, represents the probability that electron states in the metal with energy, ϵ, are vacant. $W(\epsilon,d)$ is the probability that an electron with energy, ϵ, will penetrate a potential energy barrier of thickness d.

It will be shown below that the $S(\epsilon)$ function can be removed from the integral and placed in front of it, in which case the discussion of the current will be based on the following rate expression which holds for a constant electrode potential, and hence for a constant electron energy at the Fermi level

$$i(E) = k \int_\epsilon N(\epsilon)[1 - f(\epsilon)]W(\epsilon,d)d\epsilon \qquad [9]$$

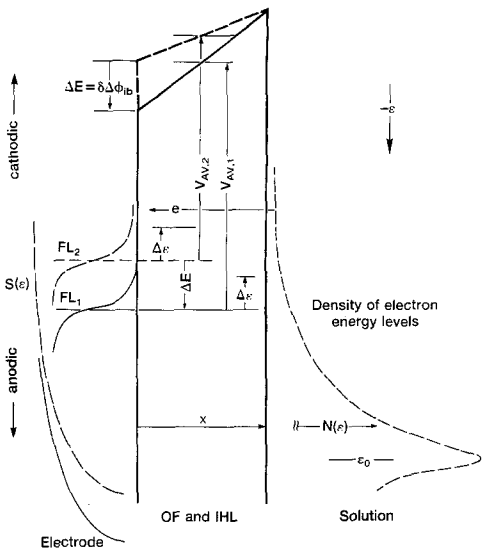

Fig. 3. A model for electron tunneling across the OF and IHL barrier for two values of electrode potential, E. As the potential increases 120 mV, the electron energy at the Fermi level, FL, of the metal decreases 120 mV, and the average barrier height, V_{AV}, which is determined from the FL, increases 60 mV. At the same time, the density of electron states in solution, $N(\epsilon)$, at the FL, and at any $\Delta\epsilon$ relative to the FL, increases ten times. This increase in $N(\epsilon)$ as E increases leads to the observed linear E-log i relationships having a predicted slope of 120 mV/dec. x is the distance from the metal/oxide film interface.

Here, k is a constant containing, among others, the $S(\epsilon)$ function. Equations [8] and [9] are written for the anodic process. The reverse, cathodic process need not be considered as the rates for the reverse process are many orders of magnitude lower (*e.g.*, 10^{10}, depending on electrode potential) than are the rates for the OER at potentials which are far removed from the reversible potential.

Each function in Eq. [9] will be analyzed in turn to determine its weight in the integration, and its effect on the rate of reaction at different potentials. Figure 3 depicts the potential energy barrier for electron tunneling at an oxide-covered electrode and illustrates the significance of various parameters used here.

Effect of the Tunneling Probability on the Reaction Rate

The probability function can be analyzed using the WKB-Gamov approximation (28, 30). For electrons in the donor species with energies $\Delta\epsilon$ above, or below, the electron energy at the Fermi level in the metal electrode, ϵ_F, it is

$$W(\Delta\epsilon,d) = \exp\left\{[-4\pi(2m_e)^{1/2}/h] \cdot \int_0^d [V(x) - \Delta\epsilon]^{1/2}\, dx\right\} \qquad [10]$$

$V(x)$ is the height of the potential energy barrier, also measured with respect to ϵ_F, experienced by a tunneling electron at a distance x from the metal/oxide film interface (Fig. 3). Coordinate x extends up to the IHP. It is assumed that all reacting donor species are effectively located at the IHP at the same distance from the metal surface. The constant m_e is the mass of an electron.

Since $V(x)$ is not known, following the common practice, it is approximated by the following linear expression [cf. (26, 28, 29)]

$$V(x) = V_{x=0} + \frac{e_o\Delta\phi_{ib}}{d} x \qquad [11]$$

Here, $V_{x=0}$ is the height of the potential energy barrier at $x = 0$. Since $\Delta\phi_{ib}$ changes with electrode potential (cf. Eq. [3]), both $V(x)$ and $W(\Delta\epsilon,d)$ also vary with the electrode potential. As the electrode potential increases, the energy of the Fermi level with respect to the electron energy in vacuum moves toward lower energies, as illustrated in Fig. 3.

Since $V_{x=0}$ is defined[2] with respect to the Fermi level of the metal, it remains constant at all potentials. However, as the electrode potential increases, the slope of $V(x)$ also increases and this leads to an increase in $V(x)$ at any other distance from the metal/inner barrier interface. Consequently, as $V(x)$ increases the probability for the same $\Delta\epsilon$ decreases (see Eq. [10]). Contrary to this, for any constant value of ϵ referred to the electron energy in vacuum, and not to the Fermi level, the probability increases as the electrode potential increases. The former dependence of $W(\Delta\epsilon)$ on electrode potential tends to decrease, the rate of the OER as the electrode potential increases. However, since the rate of the OER increases with the electrode potential, other parameters in Eq. [9] must lead to an increase in the rate of reaction as the electrode potential increases, and must show a much stronger dependence on electrode potential than $W(\Delta\epsilon,d)$ does.

It will be shown below that the major function determining the dependence of the reaction rate on electrode potential is $N(\epsilon)$. This function increases exponentially with the electrode potential and by itself gives an E-log i relationship with an 'ideal,' potential-independent, Tafel slope dE/d log i of $2.3RT/(\beta F)$, providing β is invariant with E. The decrease of $W(\Delta\epsilon,d)$ with increasing electrode potential, which is discussed in the preceding paragraph, is then expected to be algebraically added to the increase in the rate arising from $N(\epsilon)$ and in that way to modify the 'ideal' Tafel slope. As the potential increases, the slope should become larger than predicted for the 'ideal' slope. Only if $W(\Delta\epsilon)$ decreases exponentially with E will the Tafel slopes remain constant and independent of E. Since the observed Tafel slopes are so close to the 'ideal' slope, and since no change in slopes with electrode potential is observed, it follows that $W(\Delta\epsilon)$ is a very weak function of E and that it varies nearly exponentially with the electrode potential (see below). To verify this, the dependence of $W(\Delta\epsilon,d)$ on $\Delta\epsilon$ and E, and the effect of $W(\Delta\epsilon,d)$ on the rate of the OER and the Tafel slope, can be estimated in the following way. If $V(x)$ for a given electrode potential is replaced by an average barrier height, V_{AV}, above the Fermi level (cf. Fig. 3), which is also a common practice in studies of electron tunneling, then Eq. [10] becomes

$$W(\Delta\epsilon,d) = \exp\left[-4\pi d(2m_e)^{1/2}(V_{AV} = \Delta\epsilon)^{1/2}/h\right] \qquad [12]$$

As expected, at constant d, the larger V_{AV}, the lower is the probability that an electron with energy ϵ_F (*i.e.*, for $\Delta\epsilon = 0$) will penetrate the potential energy barrier. For electrons with energies above the Fermi level, (*i.e.*, for $\Delta\epsilon > 0$), $W(V_{AV},d)$ is higher than for $\Delta\epsilon = 0$. However, even in this case when $\Delta\epsilon$ is much less than V_{AV}, *i.e.*, for high potential energy barriers. $W(\Delta\epsilon,d)$ is essentially unaffected by $\Delta\epsilon$, and $\Delta\epsilon$ in Eq. [12] can be omitted and still have a fairly accurate estimate of the value for $W(\Delta\epsilon,d)$. Moreover, for high energy barriers, the changes in V_{AV} by $e\Delta E/2$ when the electrode potential increases by ΔE is usually small and an additional level of approximation is introduced by regarding $W(V_{AV},d)$ as independent of electrode potential (see below). In view of this, $W(\epsilon,d)$ in Eq. [9] can be placed in front of the integral sign.

The dependence of the rate of the OER on the barrier thickness arises solely from $W(\Delta\epsilon,d)$ (cf. Eq. [2], [9], and [16]). None of the other functions in Eq. [9] depends on d. Therefore, the exponent in Eq. [12] can be compared directly with the exponent containing d in the experimental rate equation (Eq. [2]). In the approximation that $\Delta\epsilon$ is small compared to V_{AV}, this comparison leads to

$$\frac{4\pi d(2m_e)^{1/2}V_{AV}^{1/2}}{h} = \frac{mFq}{2RT} = \delta d \qquad [13]$$

Parameters m and δ have been experimentally determined (13, 17, 19). Since V_{AV} changes with electrode potential, neither δ nor m are expected to be constant, but rather they should increase as E increases. However, no such increase in δ and m has been detected experimentally [cf. (1, 13)]. This shows that although V_{AV} increases with E even over several hundred mV's (see Eq. [15]), V_{AV} is so large that the increment in V_{AV} does not noticeably affect $V_{AV}^{1/2}$, as discussed in the previous paragraph.

From ellipsometric studies of oxide film growth at current densities of 1.5×10^{-5} A/cm^2 and 1.5×10^{-4} A/cm^2, Ward *et al.* found $\delta = 1.7$ Å^{-1} (17, 19). Using this value, Eq. [13] yields $V_{AV} = 2.75$ eV for this current density region. The potential of the Pt electrode in this region is about 1.65 V *vs.* RHE (see Fig. 2). In rotating ring-disk studies, m (~300 VC^{-1} cm^2) and q (2 mC/cm^2) corresponding to a thickness of the oxide film of about 10 Å were determined (13). With these parameters, V_{AV} for the same current density region is calculated to be 2.90 eV, which is in close agreement with V_{AV} obtained from the ellipsometric data. With $V_{AV} = 2.85$ eV at 1.65 V, $W(\Delta\epsilon = 0, d = 10$ Å) is 3.1×10^{-8}. The significance of this very low value for W will be discussed further below.

To check the earlier assumption that $\Delta\epsilon$ does not significantly affect $W(\Delta\epsilon,d)$, and that it can be omitted from Eq. [12], $W(\Delta\epsilon,d)$ is calculated for the same values of d and V_{AV}, as in the preceding paragraph, but at varying values of $\Delta\epsilon$. Assuming, for example, that $\Delta\epsilon = 0.240$ eV, *i.e.*, that an electron tunnels from an energy level 240 mV above the Fermi level, Eq. [12] then yields $W(\Delta\epsilon = 0.24, d = 10$ Å$) = 6.5 \times 10^{-8}$. Thus, the probability function increases by a factor of two as $\Delta\epsilon$ increases by 240 meV. However, as will be seen below, for the same increase in $\Delta\epsilon$, the number of electrons available for tunneling decreases by two orders of magnitude. This small change in W for a large change in electron energy justifies the omission of $\Delta\epsilon$ in Eq. [12].

It is seen from Fig. 3 that as $\Delta\phi_{ib}$ changes by $\delta(\Delta\phi_{ib})$, V_{AV} changes by

$$\Delta V_{AV} = 1/2[e\delta(\Delta\phi_{ib})] \qquad [14]$$

Since $\delta\Delta\phi_{ib}$ is equal to ΔE (cf. Eq. [3])

$$\Delta V_{AV} = 1/2[e\Delta E] \qquad [15]$$

This relationship is used above to calculate V_{AV} and will be used below in the analysis of the dependence of $W(V_{AV})$ on E.

With $V_{AV} = 2.85$ eV at $E = 1.65$ V and $\Delta\epsilon = 0$, the dependence of $W(V_{AV},d)$ on electrode potentials can be explored. In Fig. 4, a plot of log $W(V_{AV},d)$ *vs.* V_{AV} is shown for $d =$ 10 Å, and for V_{AV} in the range 2.85 ± 0.180 eV. This range corresponds to the span of electrode potentials from 1.29 to 2.01 V, *i.e.*, 360 mV above and below the test potential of 1.65 V. It is calculated that $W(V_{AV},d)$ over this potential range decreases by a factor of 3. Experimentally, over the same potential range, the rate of the OER increases by six orders of magnitude. This clearly shows that $W(V_{AV},d)$ is only a very slowly varying function of E.

The second derivative of log $W(V_{AV},d)$ with respect to V_{AV}, and hence with respect to E, is greater than zero and

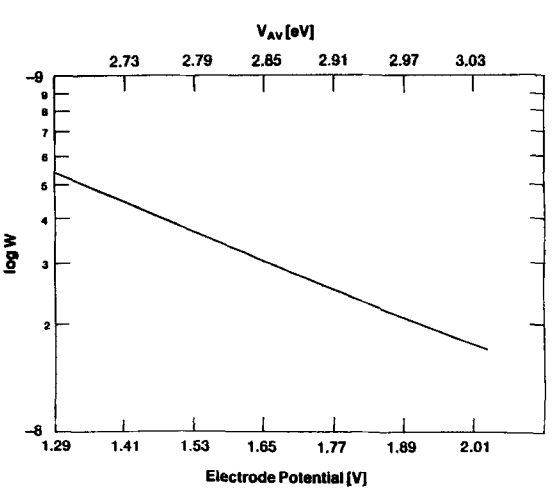

Fig. 4. The dependence of the probability function, $W(V_{AV},d)$, on the height of the potential energy barrier, V_{AV}, when the barrier thickness, d, is constant (=10 Å). The span of V_{AV} from 2.67 to 3.03 eV corresponds to the range of electrode potential, E, from 1.29 to 2.01 V *vs.* RHE. Note, $W(V_{AV},d$ = const) decreases as E increases.

[2] Here and in other works on similar subject.

consequently the log W *vs.* E lines are expected to be concave down. The Tafel lines in the E *vs.* log i plot, should then be concave up. However, in a narrow range of V_{AV} log $W(V_{AV})$ is nearly linear with E, and therefore no deviation of Tafel lines from linearity is either expected or observed. Nevertheless, because W decreases with E, the magnitude of the Tafel slope is altered by the change in W. For example, a decrease in W by a factor of 3 when E increases from 1.29 to 2.01 V should cause the Tafel slope to increase by *ca.* 9 mV per decade of current density, as compared to the value that would be expected if W were independent of E. Thus, assuming that the Tafel slope with a potential-independent $W(V_{AV},d)$ is 120 mV/dec, the slope with a potential-dependent $W(V_{AV},d)$ should be about 129 mV/dec of current density. Since the probability function contributes only 9 mV/dec, and since the Tafel slope is experimentally found to be close to 120 mV/dec, it follows that the symmetry factor, β, is not 1/2 but is slightly higher, *i.e.*, [120/(120-9)] $\times$ 0.5 = 0.54.

$W(V_{AV},d)$ has been calculated for five barrier thicknesses, *i.e.*, 6, 8, 10, 12, and 14 Å, has a function of V_{AV} (Fig. 5). It is seen that as d increases $W(d)$ at any V_{AV} decreases sharply. More significantly, however, d log W/dV_{AV} increases (in absolute values) as d increases. In view of the foregoing discussion, this means that the correction to the Tafel slopes is smaller for a thin barrier than it is for a thick one. In other words, for the same β electrodes with thicker barriers should have higher Tafel slopes than electrodes with thinner ones. No clear evidence for such deviations of the Tafel slopes with thickness of the oxide film has been reported for Pt electrodes [cf. (7)]. Carefully conducted experiments with controlled oxide film thicknesses may be required here.

Role of the Electron Energy Level Distribution in Solution and the Fermi Function on the Rate of the OER

For the distribution function, $N(\epsilon)$, of the occupied electron energy levels associated with the reacting species at the IHP, the following expression originally suggested by Gurney (24) is used in this study

$$N(\epsilon) = N(\epsilon_o) \exp[-\beta(\epsilon - \epsilon_o)/(kT)] \quad [16]$$

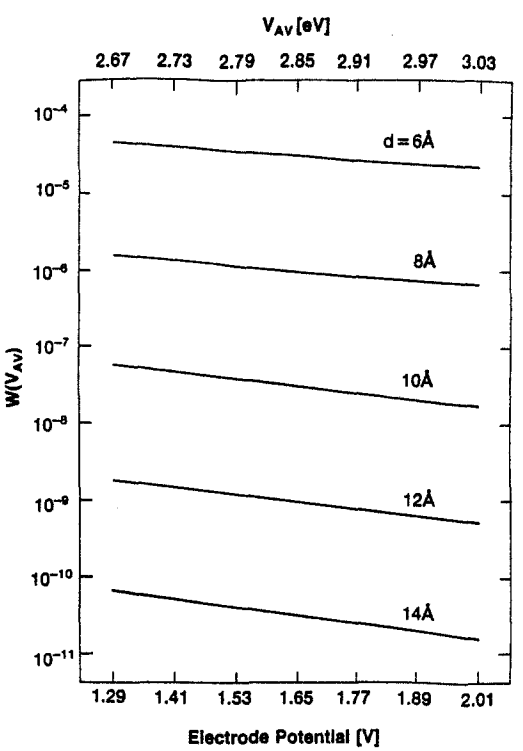

Fig. 5. The same as in Fig. 4 but for d = 6, 8, 10, 12, and 14 Å. At the same E, and hence at the same V_{AV}, $W(V_{AV})$ decreases sharply as d increases. For small thicknesses, the variation in $W(V_{AV})$ is less pronounced than for larger thicknesses.

$N(\epsilon_o)$ is the normalized dimensionless density of states having ground state energy ϵ_o with respect to the electron energy in the vacuum (Fig. 3). The Fermi function, $f(\epsilon)$, for the occupied electron states in the metal is given by

$$f(\epsilon) = \frac{1}{1 + \exp\dfrac{\epsilon - \epsilon_F}{kT}} \quad [17]$$

where ϵ_F is the energy of the electrons at the Fermi level of the metal electrode.

When $N(\epsilon)$ and $f(\epsilon)$ are introduced into Eq. [9], the following rate equation is obtained

$$i = k' \int_{-\infty}^{+\infty} \exp[-\beta(\epsilon - \epsilon_o)/(kT)]\{\exp[(\epsilon_F - \epsilon)/(kT)] + 1\}^{-1} \quad [18]$$

where k' contains, among other factors, $W(V_{AV})$ and $N(\epsilon_o)$. This equation can be integrated analytically between finite limits, and it can be shown that, over large limits of integration, the numerical value of the integral does not change significantly. The ratio of the currents obtained when the integration is carried out from ϵ_o to $\epsilon >> \epsilon_F$, and from ϵ_F to $\epsilon >> \epsilon_F$ is only $\pi/2$. One reason for this is that, at any temperature, a nearly equal number of vacant levels are available below the Fermi level as there are occupied levels above it, and the contribution to the total current from energy levels $\pm kT$ outside the Fermi level is negligible. It is therefore sufficient to integrate only from ϵ_F to evaluate the dependence of the current on E for a given d.

When the dependence of current density on ϵ_F (or on E) is sought, the dependence on the Fermi function can also be removed from the integral, provided the integration is carried out from ϵ_F. Integration with this approximation compared to integration with the Fermi function included in the integral leads to the same exponential rate equation, although with a different value of the pre-exponential factor (which is potential independent). This is because $f(\epsilon)$ shifts in harmony with E. As E increases, *e.g.*, by $\pm 2.3(2RT/F)$, the number of electrons transferred per unit time from each electron level in solution increases by about factor 10.

The following rate equation for a given ϵ_F is now obtained from Eq. [18]

$$i = k^o \exp[-\delta d] \exp[-\beta(\epsilon_F - \epsilon_o)/(kT)] \quad [19]$$

where k^o contains the concentration terms of the reacting species, which is approximately given by $N(\epsilon_o)$, and all other constants discussed above. It also contains the remaining constant parameters of $W(V_{AV},d)$. However, k^o is not a function of pH. It should be emphasized that ϵ_F, which is the electron energy with respect to the vacuum at the Fermi level, changes with the electrode potential. It decreases as electrode potential increases (see Fig. 3). The next step is to relate ϵ_F to an electrode potential.

It is sufficient to relate only one electron energy level in the electrode to an electrode potential. Following Lohmann (31) and Gerischer (32), electron energy at the Fermi level of the standard hydrogen electrode is -4.5 eV. The Fermi level energy at the potential E *vs.* SHE is then given by

$$\epsilon_F = -eE + \epsilon_{F,SHE} \quad [20]$$

where $\epsilon_{F,SHE}$ is the electron energy at the Fermi level of the SHE.

Introducing ϵ_F from Eq. [20] into Eq. [19], it is obtained

$$i = k^o \exp[-\delta d] \exp[\beta(\epsilon_o - \epsilon^o_{F,SHE})/(kT)] \exp\left[\frac{\beta FE}{RT}\right] \quad [21]$$

Since Eq. [19] is derived without taking into account the dual barrier model, and since in this model only a part of E, namely, $E - E_o$, operates across the inner barrier and can be regarded as the operative electrode potential,[3] E in Eq. [21] is now replaced with $E - E_o$. This replacement yields

[3] In the sense that only this part controls the change of current density with electrode potential at a given pH.

$$i = k \exp[-\delta d] \exp\left[\frac{\beta F(E - E_o)}{RT}\right] \quad [22]$$

Here, factors with electron energies are included into the constant k.

It should be emphasized that in the double-barrier model E_o represents the potential difference across the OHL, where the parallel process to electron transfer through the oxide film, the proton transfer occurs. This latter process is fast, in quasiequilibrium, and as such the net rate across the OHL at a given pH is potential independent. Nevertheless, and just because of this equilibrium, the potential across the OHL and hence, E_o, decrease (by $2.3RT/F$) as pH increases by one unit (see Eq. [7]). This potential difference operates outside the rate-determining reaction zone, *i.e.*, outside the inner barrier zone, and therefore should be eliminated from the rate equation which is solely controlled by the processes in the inner barrier zone.

Returning to Eq. [22], it can be seen that for a constant d, and with the symmetry factor close to 1/2, this rate equation leads to the observed rate equation for the OER and gives a Tafel slope of *ca.* 120 mV/dec of current density. The observed exponential dependence of i on d then arises only from the dependence of $W(V_{AV},d)$ on d.

Equation [22] appears to indicate the zero reaction order with respect to H_3O^+. However, since E_o measured with respect to a pH-independent reference electrode changes with pH according to Eq. [7], the current as given by Eq. [22] becomes pH dependent. Combining Eq. [7] and [22] one finally obtains

$$i = K[H_3O^+)^{-\beta} \exp[-\delta d] \exp\left[\frac{-\beta F E_{o,pH=0}}{RT}\right] \exp\left[\frac{\beta FE}{RT}\right] \quad [23]$$

and with $\beta \approx 1/2$

$$i = A[H_3O]^{-1/2} \exp[-\delta d] \exp\left[\frac{FE}{2RT}\right] \quad [2]$$

which is the rate equation experimentally observed.

In the present model, the pH dependence of the OER is linked to the change of the potential difference across the OHL. With ϕ in solution independent of pH, ϕ_{IHP} decreases as pH increases, and with respect to a pH-independent reference electrode, $E_o(=\phi_{IHP}-\phi_{sol})$ becomes pH dependent. It may be noted that this dependence of E_o on pH is formally equivalent to the change of potential in an outermost interfacial layer facing the electrode surface due to acid-base equilibria [cf. (33)]. The observed pH dependence of the OER at Pt electrodes in acid solutions is, therefore, not directly due to the participation of H_3O^+ in the rate-determining step. Rather, it is due to the change of potential outside the rate-controlling reaction zone.

The distribution function $N(\epsilon)$ is judiciously selected in this work as no other function will allow for the linear E-log i relation which is experimentally observed. This function with $\beta \approx 1/2$ yields for the first step as rate-determining a Tafel slope close to 120 mV. In this model, Tafel slopes are only insignificantly modified by the probability function, $W(\epsilon,d)$, which also accounts for the dependence of the reaction rate on the thickness of the oxide film.

The Exchange Current Density at Oxide Film Covered Electrodes

The major reason why the OER at Pt electrodes is a slow reaction, as compared to many other reactions at the same electrode, is the presence of the insulating Pt oxide film, which together with the IHL controls the tunneling probability. With $\delta = 1.7$ Å^{-1}, $W(d)$ for an oxide film 10 Å thick is about 4×10^{-8}. For such electrodes, the exchange current density is about 10^{-10} A/cm^{-2}. It follows that, could the oxide film be eliminated, the exchange current density would be about 2×10^{-3} A/cm^{-2}. This rate is comparable to the rates of some redox reactions and of the hydrogen reaction at Pt electrodes and suggests that the same basic mechanism for charge transfer is operative in all of these cases. It should be noted that the rate of the OER is not controlled by the tunneling process itself, which is a fast process, but by the requirements to bring the reacting species from the ground state in solution to the activated states, *i.e.*, by $N(\epsilon)$.

Additional Comments

Charge transfer during the OER at an electronically insulating oxide film covering an electrode is depicted in Fig. 3. As E increases, *e.g.* by 120 mV, the Fermi level (and the bottom of the conduction band) decreases by 120 meV relative to the electron energy associated with the reacting water molecules at the IHP. Thus, more electrons from the occupied levels in the solution can tunnel to the vacant electron levels in the metal. As E increases by 120 mV and the energy at the Fermi level with respect to the vacuum decreases by 120 meV, the number of electrons with energy $\Delta\epsilon$ above (or below) the Fermi level increases (decreases) ten times.

The partial currents associated with the charge transfer from any level then increases (decreases) by a factor of ten, and therefore the total current increases (decreases) ten times. This shows that, at a constant film thickness, $N(\epsilon)$ is the dominant factor in determining the change of rate of the OER with E, and it controls the Tafel slope. The Fermi distribution function affects the current in the same manner at all potentials and therefore does not affect the Tafel slope. The $S(\epsilon)$ function also moves in harmony with electrode potential and affects the current at all potentials in the same way. For this reason, it is removed from the integration. $W(\epsilon,d)$ affects the magnitude of the current density but that effect is close to be independent of electrode potential. Therefore, the Tafel slope is basically independent of the electrode potential and the oxide film thickness.

Vetter and Schultze studied the OER at Pt electrodes in some detail (4, 29). They used potentiostatic pulses to determine the current for oxygen evolution as function of the electrode potential, and coulometrically determined the thickness of the oxide film. The Tafel slopes in their work are greatly affected by the oxide film thickness and electrode potential. For thin films, *e.g.*, ≤6 Å, the slope is 90 mV/dec, *i.e.*, β is greater than 0.5. For thicker films at low potentials, the slopes are close to 120 mV/dec, *i.e.*, β = 0.5. However, as the potential increases, β increases from 0.5 to *ca.* 0.63. Both observations are at variance with the results of other workers (1-3, 6-11), which have shown that the Tafel slope is close to 120 mV over a number of decades of current densities. They are at variance also with the present analysis, which shows that the Tafel slopes should not be greatly affected by the oxide film thickness, and that they are basically independent of the electrode potential. These differences in the experimental data are most likely due to different measurement techniques and changes in the thickness of the oxide film during the determination of a single E-log i relationship. They may also be related to the much higher current densities to which the Tafel lines in Vetter and Schultze's experiments were extended (up to 1 A/cm^{-2}), perhaps leading to a change in characteristics of the Pt oxide film.

Vetter and Schultze (29) considered a similar model of charge transfer through the oxide film as used in this work, and calculated the dependence of current density on E. In contrast to the present work, they assumed that the distribution of the donor electron energy levels in solution is Gaussian, and using a parabolic approximation, they obtained

$$\beta = RT/F \; d \ln i/dE$$
$$= -2(\epsilon - \epsilon^o_{donor})e_o/(4E_{reorg})$$
$$= -2(\eta - E_{reorg})e_o/(4E_{reorg}) \quad [24]$$

Here, $E^o_{donor} = E_{reversible} + E_{reorg}/2$, E_{reorg} being the donor reorganization energy, given as 1.8 eV, and η is the overpotential for the OER. It follows that only at $\eta = 0$ and $\beta = 0.5$, *i.e.*, only at low potentials, is the Tafel slope expected to be close to 120 mV/dec. As η increases, β should decrease and the Tafel slope should increase. For instance, at $\eta = 0.6$ V, it is expected that $\beta = 0.33$ and the slope should be about

180 mV/dec. Even with a smaller E_{reorg}, the slope should increase noticeably above 120 mV/dec, which is not observed in their own experiments. It was pointed out by Gilroy that the theoretical equation based on a Gaussian distribution involves the product $d\sqrt{E}$ in the exponential, whereas the experimental results of Vetter and Schultze preclude an interaction term of this type (34).

In the derivation of the rate equation for the OER at oxide-covered electrodes, Schmickler (35) expanded the square root in the WKB-Gamov approximation and obtained an expression for the tunneling probability. It follows from that expression that the probability decreases exponentially as the electrode potential increases. From his rate expression, β is given by

$$\beta = 1/2 - \frac{2kTd(2m_e)^{1/2}}{hV_B^{1/2}} \quad [25]$$

where V_B is the average barrier height above the Fermi level at zero overpotential, and other symbols have the same significance as above. It follows that as d increases, β should decrease and, hence, the Tafel slope should increase. An increase in the Tafel slope with film thickness was reported by Vetter and Schultze (4, 29). In the current density region from about 3×10^{-5} A/cm^2 to 3×10^{-1} A/cm^2, they reported a slope of 90 mV/dec for $d = 4.9$ Å, and a slope of 120 mV/dec for $d = 7.1$ Å at low current densities. However, at both thicknesses, $\beta \geq 1/2$. This change of slopes with the oxide film thickness is not in accord with Eq. [25], which predicts that at any thickness and at all potentials, $\beta < 1/2$, *i.e.*, the Tafel slopes should always be greater than 120 mV/dec.

Manuscript submitted Dec. 12, 1990; revised manuscript received April 3, 1990.

Allied-Signal, Inc., assisted in meeting the publication costs of this article.

REFERENCES

1. V. I. Birss and A. Damjanovic, *This Journal*, **130,** 1694 (1983).
2. J. O'M. Bockris and A. K. M. Shakshul Huq, *Proc. R. Soc. London*, **A237,** 227 (1956).
3. I. A. Hickling and S. Hill, *Trans. Faraday Soc.*, **46,** 550 (1950).
4. J. W. Schultze and K. J. Vetter, *Electrochim. Acta*, **18,** 889 (1973).
5. I. I. Pushnograeva, A. M. Skindin, Yu. B. Yasil'ev, and B. S. Bagotskii, *Sov. Electrochem.*, **6,** 134 (1970).
6. A. Damjanovic, A. Dey, and J. O'M. Bockris, *Electrochim. Acta*, **11,** 791 (1966).
7. A. Damjanovic and B. Jovanovic, *This Journal*, **123,** 374 (1976).
8. D. V. Kokoulina, Yu. I. Krasovitskaya, and L. I. Kritshtalik, *Sov. Electrochem.*, **7,** 1172 (1971).
9. G. N. Afonshin, G. F. Volodln, and Yu. M. Tyurin, *ibid.*, **7,** 1295 (1971).
10. J. P. Hoare, *This Journal*, **112,** 602 (1965).
11. E. I. Krushcheva, O. V. Morovskaya, N. A. Shumilova, and B. S. Bagotskii, *Elektrokhimiya*, **8,** 205 (1972).
12. M. R. Tarasevich, A. Sadowskl, and E. Yeager, in "Comprehensive Treatise of Electrochemistry," Vol. 7, p. 301, Plenum Press, New York (1983).
13. V. I. Birss and A. Damjanovic, *This Journal*, **130,** 1688 (1983).
14. T. Erdey-Gruz and O. Golopentza-Bajor, *Acta Chim. Hung.*, **34,** 281 (1962).
15. K. J. Vetter and J. W. Schultze, *J. Electroanal. Chem.*, **34,** 131, 141 (1972).
16. J. L. Ord and F. C. Ho, *This Journal*, **118,** 46 (1971).
17. A. Damjanovic, A. T. Ward, B. Ulrick, and M. O'Jea, *ibid.*, **122,** 471 (1975).
18. A. T. Ward, A. Damjanovic, E. Gray, and M. O'Jea, *ibid.*, **123,** 1599 (1976).
19. A. Damjanovic, A. T. Ward, and M. O'Jea, *ibid.*, **121,** 1186 (1974).
20. A. Damjanovic and L-S. R. Yeh, *ibid.*, **126,** 555 (1979).
21. R. E. Meyer, *ibid.*, **107,** 847 (1960).
22. J. J. MacDonald and B. E. Conway, *Proc. R. Soc. London, Ser. A*, **269,** 419 (1962).
23. K. E. Heusler and K. S. Yun, *Electrochim. Acta*, **22,** 977 (1977).
24. R. W. Gurney, *Proc. R. Soc. London, Ser. A*, **134,** 137 (1931).
25. H. Gerischer, *Z. Phys. Chem. NF*, **26,** 223 (1960).
26. D. B. Mathews and J. O'M. Bockris, in "Modern Aspects of Electrochemistry," B. E. Conway and J. O'M. Bockris, Editors, Vol. 6, p. 242, Plenum Press, New York (1971).
27. S. U. M. Khan and J. O'M. Bockris, *This Journal*, **132,** 2648 (1985).
28. J. O'M. Bockris and S. U. M. Khan, "Quantum Electrochemistry," Plenum Press, New York (1979).
29. K. J. Vetter and J. W. Schultze, *Ber. Bunsenges. Phys. Chem.*, **77,** 945 (1973).
30. D. Bohm, "Quantum Theory," p. 275, Prentice Hall, Inc., Englewood Cliffs, NJ (1951).
31. F. Lohmann, *Naturforsch.*, **22a,** 843 (1967).
32. H. Gerischer, National Bureau of Standards, Special Publication, Vol. 455, p. 1 (1976).
33. S. Trasatti, in "Advances in Electrochemistry and Electrochemical Engineering," H. Gerischer and C. W. Tobias, Editors, Vol. 10, p. 213, John Wiley and Sons, New York (1977).
34. D. Gilroy, *J. Electroanal. Chem.*, **83,** 329 (1977).
35. (a) W. Schmickler, *ibid.*, **84,** 203 (1977); (b) W. Schmickler and J. W. Schultze, *Z. Phys. Chem., N.F.*, **110,** 533 (1979).